Journal of the European Ceramic Society 21 (2001) 737–743

www.elsevier.com/locate/jeurceramsoc

Processing and electrical properties of NASICON prepared from yttria-doped zirconia precursors

R.O. Fuentes [a,b], F.M. Figueiredo [a,c,*], F.M.B. Marques [a], J.I. Franco [b]

[a] *Ceramics and Glass Engineering Department, UIMC, University of Aveiro, 3810-193 Aveiro, Portugal*
[b] *PRINSO-CITEFA-UNSAM, Buenos Aires, Argentina*
[c] *Science and Technology Department, Universidade Aberta, R. Escola Politécnica no 147, 1269-001 Lisbon, Portugal*

Received 28 May 2000; received in revised form 1 August 2000; accepted 20 August 2000

Abstract

This work reports on the synthesis and characterization of NASICON obtained from solid state reaction between SiO_2, $Na_3PO_4{\cdot}12H_2O$ and two types of zirconia: monoclinic ZrO_2 and yttria-doped tetragonal phase $(ZrO_2)_{0.97}(Y_2O_3)_{0.03}$. Powders and dense samples were characterized by SEM, XRD and DTA. Electrical conductivity was measured by impedance spectroscopy. Results obtained with different NASICON samples showed a significant role of composition and processing conditions on the electrical properties. Dense yttria-doped samples were obtained at a lower temperature than the undoped material. The electrical conductivity, close to 2×10^{-3} S cm^{-1} at room temperature, is significantly higher than the value obtained with the material prepared from pure ZrO_2. Attempts to compensate the charge unbalance due to replacement of Y^{3+} for Zr^{4+} with additions of Na^+ failed. Instead, a drop in electrical conductivity due to an enhancement of the grain boundary impedance was observed. Formation of monoclinic zirconia and glassy phases along the grain boundary were responsible for this effect. Results suggest a major role of microstructure on electrical properties rather than composition.

Keywords: Impedance spectroscopy; Ionic conductivity; NASICON; Solid state reaction

1. Introduction

Oxides with the general formula $Na_{1+x}Zr_2Si_xP_{3-x}O_{12}$ $(0<x<3)$ are well known as NASICON, Na super ionic conductors.[1,2] Due to a high ionic conductivity and claimed stability under conditions of practical relevance,[3] NASICON thin or thick films have been suggested as ion selective electrodes or gas sensor devices.[4–6]

The structure of these materials can be seen as a three dimensional arrangement of ZrO_6 octahedra linked to SiO_4 or PO_4 tetrahedra by corner shared oxygens. The Na^+ ions are located in the interstitial sites formed by this three dimensional network. Conduction happens when Na^+ moves from one interstitial site to another through "bottlenecks" formed by a triangle of oxygen ions.

One important characteristic of this family of materials is a wide range of stoichiometries, where x can virtually assume any value between 0 and 3. Thus, a number of compositions with different structural and electrical properties are possible. The highest ionic conductivity in undoped materials is observed in the monoclinic structure, obtained for $x\approx2$.[7] Partial replacement of either of the original cations has been widely exploited in numerous works aiming at improved properties.[8–10]

Composition affects the electrical behavior of the material but processing also has a key role, as very reactive powders are needed. The sintering temperature must be high enough to obtain total combination of reactants and, simultaneously, low enough to avoid loss of Na-or P-based volatile compounds and, consequently, segregation of monoclinic zirconia in the grain boundary, with a blocking effect on charge transport.[3] The ceramic route, based on solid state reaction of oxide or carbonate precursors at relatively high temperatures, yields low reactivity powders with relatively large grain size, and has therefore been questioned. The alternative sol–gel route has proven to be a successful technique in

* Corresponding author at: Ceramics and Glass Engineering Department, UIMC, University of Aveiro, 3810-193 Aveiro, Portugal. Tel.: +351-3427-0263; fax: +351-3425-300.
E-mail address: framos@cv.ua.pt (F.M. Figueiredo).

0955-2219/01/$ - see front matter
PII: S0955-2219(00)00264-8

processing of performant materials. In fact, the sol–gel procedure, based on hydrolysis–polycondensation reactions of alkoxides in alcohol medium, with excess of water and under strong stirring, yields very fine and reactive powders.[11,12] However, the cost of a sol–gel route is a serious drawback.

Previous work showed that the electrical properties of $Na_3Zr_2Si_2PO_{12}$ materials obtained via a ceramic route could be considerably improved by using a highly reactive zirconia precursor, the well known 3 mol% yttria-doped tetragonal polycrystalline zirconia (TZP).[13] The main expected advantage was a significant increase in the reaction kinetics at low temperature, not only due to the smaller particle size but also because of the low stability of the zirconia tetragonal phase. The identification of possible defects created to compensate for the charge unbalance (due to replacement of Y^{3+} for Zr^{4+}) was ignored before. In this work, the study is extended to compositions with excess of Na^+ added to compensate for the charge unbalance.

2. Experimental procedures

Three kinds of NASICON compounds were prepared:

a. NASICON, the classical $Na_3Zr_2Si_2PO_{12}$, starting from pure monoclinic ZrO_2;
b. A derived material starting from TZP as a precursor, hereby called NASICON-TZP, with a nominal formula $Na_3Zr_{1.88}Y_{0.12}Si_2PO_{12}$; and
c. NASICON-TZP-Na with an excess of Na added to compensate the charge unbalance due to replacement of Zr^{4+} by Y^{3+}, corresponding to a nominal composition $Na_{3.12}Zr_{1.88}Y_{0.12}Si_2PO_{12}$.

Powders of ZrO_2 (Riedel-de-Haën), $(ZrO_2)_{0.97}(Y_2O_3)_{0.03}$ (Tosoh), $Na_3PO_4.12H_2O$ (Merck), SiO_2 (Merck) and Na_2CO_3 (Merck), were mixed in appropriate stoichiometric ratios and ball-milled with ethanol for 2 h. After drying at 60°C, the mixtures were calcined in air at temperatures ranging from 900 to 1100°C during 8 h in order to obtain single phase materials. To obtain fine reactive powders, a second ball-milling step was introduced. This powder was then disk shaped into 1 cm diameter pellets by two consecutive pressing steps: uniaxially at 98 MPa for 2 min, and isostatically at 200 MPa for 5 min. Sintering was carried out in air at temperatures between 1230 and 1265°C for 10 h, with the pellets inside a closed Pt crucible to avoid major losses due to volatilization.

Following this procedure, dense specimens were obtained for NASICON-TZP and NASICON-TZP–Na but only poor densities could be obtained for the classical NASICON. In this case the powder with an organic binder was pressed and pre-sintered under vacuum at 900°C for 2 h, before final sintering in air at 1260°C for 16 h. A pre-calcination step under vacuum is used to eliminate the binder. Further details on this procedure can be found elsewhere.[13,14]

Structural and phase composition of powders and pellets was carried out by XRD using CuK_α radiation with a scan speed of 0.1°/min and step width, 0.02°. Powder XRD patterns were used to estimate lattice parameters. The density of the materials was determined from weight and external dimensions of the pellets. Dense pellets were polished and thermally etched at 1100°C during 10 min to enhance grain and grain boundary contrast for ulterior scanning electron microscopy (SEM) observation.

Concentration of Na and P was verified by inductively coupled plasma-mass spectrometry (ICP–MS), after each temperature treatment, for stoichiometry control. Solutions for ICP–MS analysis were prepared by dissolution of grounded pellets in an ultrasonic bath with HF.

Platinum electrodes were painted onto the surface of polished dense pellets and sintered at 700°C for 30 min. These pellets were then characterized by impedance spectroscopy between 0 and 200°C in the frequency range from 20 Hz to 1 MHz using an HP 4284A LCR meter.

3. Results and discussion

3.1. Processing conditions and phase composition

Fig. 1 shows XRD patterns of different powders calcined at two different temperatures. At low temperature (900°C), no NASICON is formed when pure monoclinic zirconia is used as precursor, but NASICON is clearly present when using TZP as source of zirconium (Fig. 1a). In both low temperature patterns, observation of uncombined reactants (ZrO_2, TZP and Na_3PO_4) shows that 900°C is not high enough for completion of the NASICON forming reaction. The patterns of similar powders calcined at 1100°C are shown in Fig. 1b. At this temperature, NASICON is clearly present in all materials. However, diffraction peaks corresponding to small amounts of monoclinic ZrO_2 and Na_3PO_4 are still present in the case of NASICON prepared from undoped ZrO_2. Reaction seems to be complete in the case of NASICON-TZP, but in the NASICON-TZP-Na composition some monoclinic zirconia is also present.

In order to check for stoichiometry deviations, the amount of Na and P were, at the different temperature steps of sample preparation, estimated by ICP–MS. Results are shown in Table 1. Na concentration estimates are slightly higher than the expected stoichiometric values. To the contrary, values for P are lower than the stoichiometric composition. Apparently, the preparation

route of the analytical solutions for ICP–MS affects Na determination. Note that errors resulting from precursors dosage are less probable because the initial Na and P concentrations are defined by the same initial reactant $Na_3PO_412H_2O$. Despite these constraints, it can be said with reasonable confidence that: (i) Na volatilization seems to be less important than P; (ii) Na and P losses increase with sintering temperature.

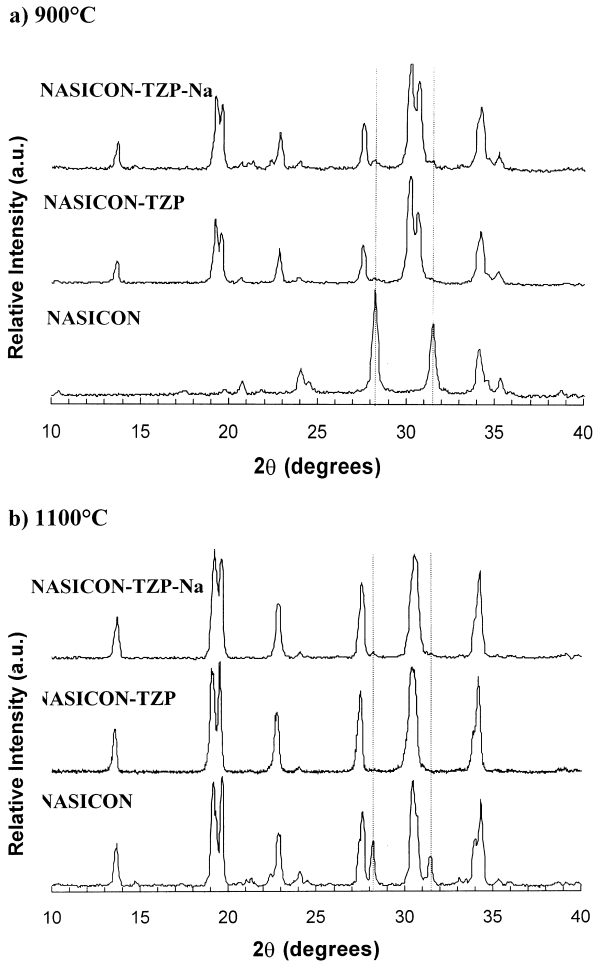

Fig. 1. XRD of calcined NASICON, NASICON-TZP and NASICON-TZP–Na powders, at (a) 900°C and (b) 1100°C. At 1100°C, the strongest lines of monoclinic ZrO_2 are not present in NASICON-TZP powders. Dashed lines show the positions of the main monoclinic ZrO_2 diffraction peaks.

Table 1
Na and P contents in the NASICON materials estimated by ICP–MS[a]

Material	Sintering T (°C)	Na (wt.%)	P (wt.%)
NASICON	1100	13.49 (12.99)	5.63 (5.84)
	1260	13.23 (12.99)	4.96 (5.84)
NASICON-TZP	1100	13.60 (13.00)	5.73 (5.84)
	1220	13.51 (13.00)	5.43 (5.84)
	1230	13.35 (13.00)	5.36 (5.84)
NASICON-TZP-Na	1100	13.73 (13.46)	5.58 (5.81)

[a] Stoichiometric values are presented inside brackets.

Previous work[15] suggested that the Na^+ concentration depends not only on the Si/P ratio but also on the Zr concentration. In this case, this family of materials should be described in the quarternary system Na_2O–SiO_2–P_2O_5–ZrO_2 by the general formula $Na_{1+z}Zr_{2-y}Si_xP_{3-x}O_{12}$, where $z-x-4y=0$. According to this relation, the introduction of 0.12 mol of Na^+ would lead to the formation of 0.5 vol.% ZrO_2, which is far below the detection limits of the diffractometer. Therefore, although thermodynamically predicted, the apparent amount of monoclinic zirconia found in the NASICON-TZP–Na powder cannot be justified by the excess of Na^+. TZP should be only partly combined. Note that the TZP main peak could be masked by the NASICON peaks in the 2θ range from 30 to 31°. Fig. 1 shows NASICON appearing before monoclinic zirconia is identified, suggesting that the entire process involves more than one stage. A first step would be the partial consumption of TZP in the reaction with the remaining precursors for the formation of the NASICON phase. The subsequent formation of monoclinic zirconia might be the result of either loss of yttrium from the unreacted TZP to the NASICON phase, or due to precipitation of ZrO_2 from the NASICON-type phase, following Na and P losses, either segregated to glassy phases or, less likely, volatized to the atmosphere. In fact, the small deviation to the stoichiometric composition found for all materials (see ICP-MS results in Table 1) suggests that most of Na and P remain in the material, presumably as glassy phases.

All three NASICON compositions could be indexed to a monoclinic structure in the space group C2/c according to JCPDS-ICDD file no. 35-412. The estimated lattice parameters are presented in Table 2. The partial replacement of Y^{3+} for Zr^{4+} provokes a lattice expansion mainly due to an increase in the a parameter of the unit cell. This fact suggests a prevailing effect of the higher ionic radius of Y^{3+} on the expected lower electrostatic repulsion due to its smaller charge.[16] Comparison between both TZP-based materials shows a decrease in the lattice volume with the introduction of excess Na^+.

Table 2
Lattice parameters estimated from XRD of powders calcined at 1100°C for 10 h[a]

Material	a (Å)	b (Å)	c (Å)	β (°)	V (Å^3)
NASICON	9.071	9.174	15.584	123.74	1078.4
NASICON-TZP	9.139	9.157	15.620	124.06	1082.3
NASICON-TZP–Na	9.115	9.150	15.637	124.08	1080.2

[a] Patterns were indexed to a monoclinic structure (space group C2/c) according to the JCPDS-ICDD file no 35-412.

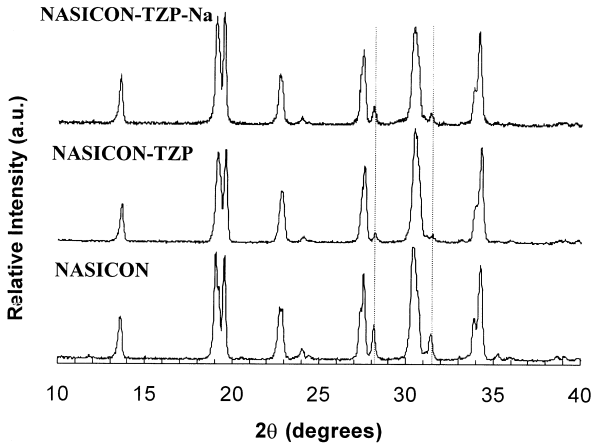

Fig. 2. XRD of NASICON-TZP–Na (1230°C), NASICON TZP (1230°C) and NASICON (1265°C) sintered pellets. Dashed lines show the positions of the main monoclinic ZrO_2 diffraction peaks.

To obtain dense samples, NASICON-TZP and NASICON-TZP–Na were sintered at 1230°C while NASICON pellets were obtained only after sintering at 1265°C XRD patterns of sintered samples of all materials are shown in Fig. 2. All of them exhibit diffraction lines typical of monoclinic ZrO_2. When compared to the patterns obtained at 1100°C (Fig. 1b), it is noticeable that there is an increase in the relative intensity of the monoclinic ZrO_2 peaks, suggesting higher amounts of this zirconia phase with increasing sintering temperature. The most probable reason for this increase is segregation from the NASICON phase due to Na and P losses.

Fig. 3 shows SEM micrographs of NASICON, NASICON-TZP and NASICON-TZP-Na sintered samples after polishing and thermal etching. NASICON exhibits heterogeneous grain size between 1 and 6 μm. The presence of liquid phase between grains is suggested

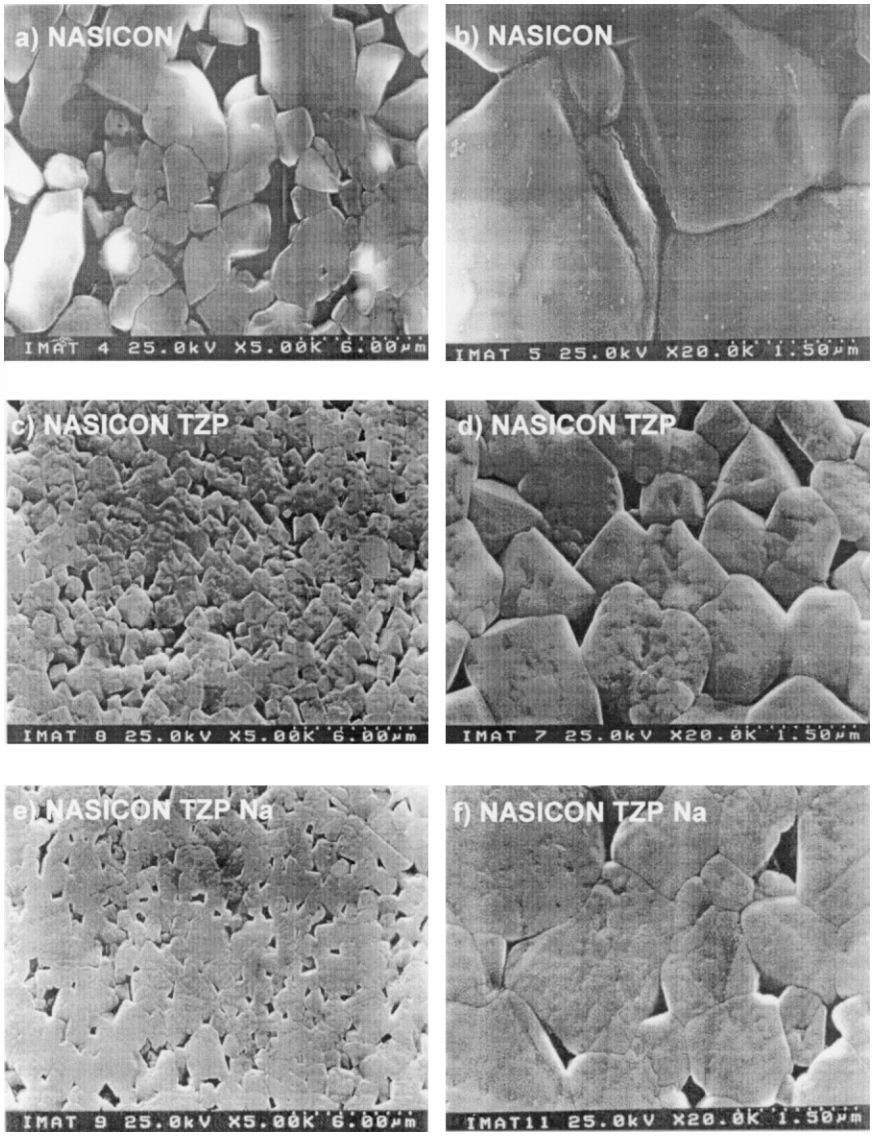

Fig. 3. SEM micrographs of NASICON-TZP–Na (1230°C), NASICON-TZP (1230°C) and NASICON (1265°C) sintered samples.

in some observations. Previously, transmission electron microscopy observations of similar compositions revealed the presence of Na and P rich liquid phases surrounding the grains of the material.[17] This is a direct consequence of the high sintering temperatures employed to get well-densified pellets, close to the melting temperature.

An homogeneous grain size of about 1 μm is evidenced in the case of NASICON-TZP pellets. A similar microstructure with slightly larger grains (about 2–3 μm) is observed in NASICON-TZP–Na pellets. No vestige for the formation of liquid phase could be noticed in either case. Simple observation of the microstructures previously presented also suggests that the densification of NASICON-TZP and NASICON-TZP–Na is higher than found for the classical NASICON composition.

Fig. 4 shows the density of pellets of the three materials sintered at different temperatures. The relevance of the sintering temperatures in the densification of NASICON is obvious. However, the higher densities are attained by the TZP-based materials, which are close to or higher than 100% of theoretical density predicted from the estimated lattice cell volume and stoichiometry (3.25 and 3.28 g/cm^3 for NASICON-TZP and NASICON-TZP–Na, respectively). This result is clearly contradicted by the observed microstructures suggesting a porosity of a few%. The presence of monoclinic zirconia peaks (Fig. 2) shows that the pellets were actually composites NASICON + monoclinic ZrO_2, besides some unidentified amount of glassy phases. If we assume that 2 vol.% of zirconia is present, the theoretical density of the mixture with 98 vol.% NASICON and 2 vol.% ZrO_2 is higher than the estimated theoretical values of NASICON-TZP and NASICON-TZP-Na. This is a direct consequence of the high density of monoclinic zirconia ($d = 5.5$ g/cm^3).[18]

3.2. Electrical properties

Fig. 5 shows the typical impedance spectra at 0°C of NASICON (sintered at 1265°C), NASICON-TZP and NASICON-TZP-Na (both sintered at 1230°C) samples. Only the grain boundary arc is clearly seen and the bulk contribution can only be estimated from the high frequency intercept of the grain boundary arc. Simple inspection of the spectra shown in Fig. 5 suggests that the major differences between these materials are mostly due to the grain boundary contribution as all high frequency intercepts of the grain boundary arc are close to each other. However, in the NASICON pellet the bulk contribution tends to be higher. At room temperature, NASICON shows a total ionic conductivity of about 4×10^{-4} S cm^{-1}, while values of about 1×10^{-3} S cm^{-1} were obtained for NASICON-TZP and NASICON-TZP–Na sintered at 1230°C.

Differences in conductivity can be relatively well understood on the basis of the structural features discussed above. The lower bulk impedance found for the TZP-based materials is coherent with the higher mobility of the Na^+ ions due to a larger cell dimensions. The increasing grain boundary resistance in the sequence NASICON-TZP/NASICON-TZP–Na/NASICON follows the relative intensity of zirconia peaks shown in Fig. 2. Presumably, the higher the peak intensity the higher the amount of segregated monoclinic zirconia + glass along the grain boundaries, both blocking the charge transport. Indeed, in the case of NASICON a generous amount of liquid phase could be identified along the grain boundaries, which is known to result in a low temperature ion-blocking behavior.

No apparent benefit arises from the additional introduction of Na^+ in NASICON-TZP-Na material. In fact, excess Na^+ might segregate to the grain boundaries as Na_2O,[17] acting as flux agent. This would explain the somewhat larger grain size of the NASICON-TZP–Na.

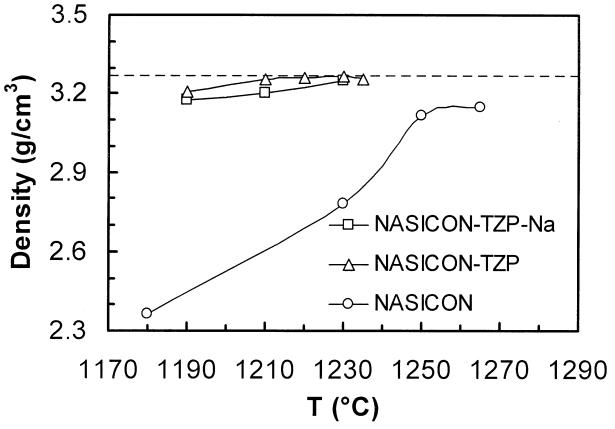

Fig. 4. Dependence of the density of NASICON pellets on sintering temperature. The dashed line shows the theoretical value for NASICON-TZP–Na.

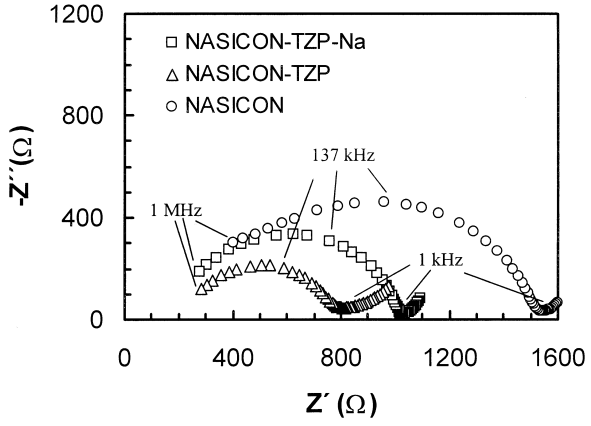

Fig. 5. Impedance spectra at 0°C of NASICON-TZP–Na (1230°C), NASICON TZP (1230°C) and NASICON (1265°C).

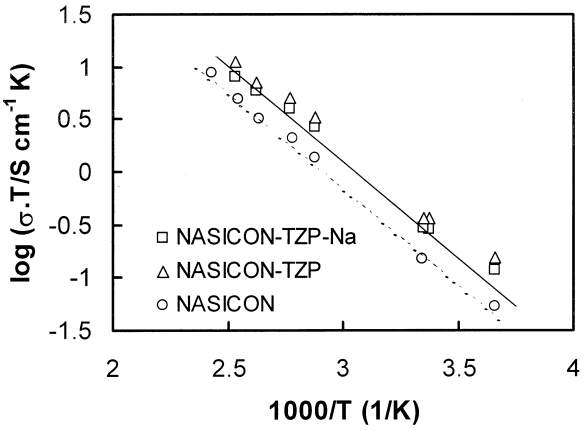

Fig. 6. Arrhenius-type plots of total conductivity (σ) as a function of absolute temperature. Activation energies estimated from these plots were 0.36 eV for NASICON sintered at 1265°C and 0.34 eV for NASICON-TZP-Na and NASICON-TZP, both sintered at 1230°C. Lines correspond to data for samples sintered at 1200°C[6] (solid line) and 1250°C[11] (dashed line) obtained following sol–gel routes.

The activation energy for total ionic conduction was estimated from the Arrhenius plot shown in Fig. 6. In the temperature range between 0 and 150°C, the activation energies calculated for NASICON (sintered at 1265°C) and NASICON-TZP/NASICON-TZP-Na (sintered at 1230°C) were 0.36 and 0.34 eV, respectively. Although the grain boundary contribution is clearly dominating the electrical performance, the small difference in the activation energies indicates similar conduction mechanisms for all materials. This result was also reported for composites of $(ZrO_2)_{0.92}(Y_2O_3)_{0.08}$ + soda-lime glass, with the activation energy for electrical conductivity being nearly independent of the glass fraction.[19]

Overall similar values were reported for similar compositions. Solid lines in Fig. 6 correspond to data obtained for NASICON samples sintered at 1200°C[6] and 1250°C,[11] with optimized microstructure, obtained following sol–gel routes. The good results now obtained with the NASICON-TZP and NASICON-TZP–Na demonstrate how promising this approach is for the development of a cheap processing route for these materials.

4. Conclusions

Due to the use of a high reactivity powder (TZP), NASICON-type materials could be processed and sintered at lower temperatures than required for the classical ceramic route using a conventional ZrO_2 powder. The major consequences of this alternative procedure were the production of dense pellets with smaller content of monoclinic zirconia, homogeneous microstructures without obvious vestiges of liquid phase, overall high electrical conductivities, and a significant benefit in the abatement of the grain boundary impedance. This reduction in grain boundary impedance and in the formation of glassy phases seems to be related to the amount of monoclinic zirconia formed during the high temperature treatments. Easy formation of glassy phases (rich in Na, Si and P oxides) and monoclinic zirconia explains why materials with only small deviations from global nominal composition show significantly different electrical performance.

Acknowledgements

Financial support from the Alfa (CEC, Brussels) and Praxis Programs (FCT, Portugal) is greatly appreciated.

References

1. Hong, H. Y. P., Crystal structures and crystal chemistry in the system $Na_{1+x}Zr_2Si_xP_{3-x}O_{12}$. *Mat. Res. Bull.*, 1976, **11**, 173–182.
2. Goodenough, J. B., Hong, H. Y. P. and Kafalas, J. A., Fast Na^+-ion transport in skeleton structures. *Mat. Res. Bull.*, 1976, **11**, 203–220.
3. Ahmad, A., Wheat, T. A., Kuriakose, A. K., Canaday, J. D. and McDonald, A. G., Dependence of the properties of NASICONs on their composition and processing. *Solid State Ionics*, 1987, **24**, 89–97.
4. Caneiro, A., Fabry, P., Khireddine, H. and Siebert, E., Performance characteristics of a sodium super ionic conductor prepared by sol-gel route for sodium ion sensors. *Anal. Chem.*, 1991, **63**, 2550–2557.
5. Ahmad, A., Glasgow, C. and Wheat, T. A., Sol-gel processing of NASICON thin-film precursors. *Solid State Ionics*, 1995, **76**, 143–154.
6. Khireddine, H., Fabry, P., Caneiro, A. and Bochu, B., Optimization of NASICON composition for Na^+ recognition. *Sensors and Actuators B*, 1997, **40**, 223–230.
7. Gordon, R. S., Miller, G. R., McEntire, B. J., Beck, E. D. and Rasmunssen, J. R., Fabrication and characterization of NASICON electrolytes. *Solid State Ionics*, 1981, **3/4**, 243–248.
8. Takahashi, T., Kuwabara, K. and Shibata, M., Solid-state ionic conductivities of Na^+ ion conductors based on NASICON. *Solid State Ionics*, 1980, **1**, 163–175.
9. Nagai, M., Fujitsu, S. and Kanazawa, T., Ionic conductivity in the system $NaZr_2(PO_4)_3$–$Na_3Y_2(PO_4)_3$. *J. Am. Ceram. Soc.*, 1980, **63**, 476–478.
10. Fujitsu, S., Nagai, M., Kanazawa, T. and Yasui, I., Conduction paths in sintered ionic conductive material $Na_{1+x}Zr_{2-x}Y_x(PO_4)_3$. *Mat. Res. Bull.*, 1981, **16**, 1299–1309.
11. Perthuis, H. and Colomban, Ph, Well densified NASICON type ceramics elaborated using sol-gel process and sintering at low temperatures. *Mat. Res. Bull.*, 1984, **19**, 621–631.
12. Colomban, Ph., Gel technologies in ceramics, glass-ceramics and ceramic-ceramic composites. *Ceram. Int.*, 1989, **19**, 23–50.
13. Fuentes, R., Franco, J. and Marques, F. B., Synthesis and properties of NASICON prepared from different zirconia-based precursors. *Bol. Soc. Esp. Cer. y Vidrio*, 1999, **38**(6), 631–634.
14. Fuentes, R. and Franco, J., Influence of the interface NASICON/electrode in the study of the conductivity. *Anales de la Asociación Química*, 1996, **84**, 287–301.
15. von Alpen, U., Bell, M. F. and Höffer, H. H., Compositional dependence of the electrochemical and structural parameters in the NASICON system ($Na_{1+x}Si_xZr_2P_{3-x}O_{12}$). *Solid State Ionics*, 1981, **3/4**, 215–218.

16. Shannon, R. D. and Prewitt, C. T., Effective ionic radii in oxides and fluorides. *Acta Cryst*., 1969, **B25**, 925–945.
17. Ramloll, C.S. *Synthesis and Properties of Yttrium and Sodium Co-doped NASICON*. MSc Thesis, University of Aberdeen, 1999.
18. Perfilyev, M. V., Demin, A. K., Kuzin, B. L. and Lipilin, A. S. In *High Temperature Electrolysis of Gases*. Nanka, Moscow, 1988.
19. Rodrigues, C. M. S., Labrincha, J. A. and Marques, F. M. B., Monitoring of the corrosion of YSZ by impedance spectroscopy. *J. Eur. Ceram. Soc*., 1998, **18**, 95–104.